

# A Quantitative Exploration of Access Point Mobility for mmWave WiFi Networks

Yubing Jian, Yuchen Liu, Shyam Krishnan Venkateswaran, Douglas M Blough, and Raghupathy Sivakumar  
Georgia Institute of Technology Atlanta, USA  
[{yubing, yuchen.liu, shyam, doug.blough, siva}@ece.gatech.edu](mailto:{yubing, yuchen.liu, shyam, doug.blough, siva}@ece.gatech.edu)

**Abstract**—mmWave is emerging as an essential technology for next-generation wireless networks due to its capability of delivering multi-gigabit throughput performance. To achieve such a promising performance in mmWave communications, Line-of-sight (LOS) connectivity is a critical requirement. In this work, we explore the strategy of infrastructure mobility to alter the location of an access point (AP) in order to provide LOS connectivity to stations (STAs) in indoor mmWave WiFi networks. Through both simulation-based and theoretical analyses, we make a detailed case for infrastructure mobility by identifying the impact of AP mobile platforms configurations on network performance and propose a ceiling-mounted mobile (CMM) AP model. Then, we compare the performance of a CMM AP with multiple static APs, and we identify that the throughput and fairness performance of a CMM AP is better than as many as 5 ceiling-mounted static APs.

**Index Terms**—Infrastructure mobility, mmWave WiFi

## I. INTRODUCTION

WiFi is a ubiquitous and impactful wireless technology. According to Cisco Visual Networking Index [1], WiFi is predicted to generate 51% of total internet traffic in 2022, and there will be nearly a 3x increase of the total amount of WiFi internet traffic from 2017 to 2022. Due to this significant increase of internet traffic generated by WiFi, there is a pressing need to improve the WiFi network performance. Among the latest WiFi related wireless technologies, mmWave is emerging as an essential technology for next-generation WiFi networks. The mmWave WiFi standard (e.g., IEEE 802.11ad) operates in the 60GHz unlicensed frequency band. It can deliver multi-gigabit ( $\sim 7\text{Gbps}$ ) performance primarily by virtue of using a large bandwidth (greater than 2GHz). Specifically, the bandwidth supported by 802.11ad is 12.5x larger than the bandwidth supported by the latest non-mmWave WiFi standard 802.11ax. While the potential performance is quite promising, mmWave is vulnerable to unreliable wireless channel conditions (especially non-line-of-sight (NLOS)) compared to conventional WiFi operating in 2.4GHz or 5GHz. The communication performance drops significantly when the wireless link has an obstacle such as a wall or a cabinet in its way. Given the fickle nature of mmWave communication, it is expected to be predominantly used in a dual-band (or a tri-band) configuration that works along with conventional WiFi.

In this context, it is likely that mmWave WiFi can deliver considerably better performance, but that the performance cannot be assured since it is dependent on the existence of

LOS conditions. As for LOS condition, it is a function of the physical environment, but communication technologies hitherto have had no ability to improve the conditions when necessary. In recent years, related works have started exploring *infrastructure mobility* as a degree of freedom in the WiFi framework that can be exploited to improve the physical environmental conditions for wireless communications [2]–[5]. Considering the strategy of infrastructure mobility, a WiFi AP with mobility can discover an optimal location for itself and move to that location to offer the best possible performance for the network. Given that mmWave WiFi has a critical requirement on wireless channel conditions, infrastructure mobility becomes an especially attractive degree of freedom for mmWave WiFi, where the creation of LOS conditions can have a profound impact on the overall network performance.

Before developing an algorithm to leverage the benefits of infrastructure mobility in mmWave WiFi, there are two fundamental questions that need to be investigated in the first place: 1) *What is the impact of various AP mobile platform configurations (e.g., platform location, orientation, and shape) on the network performance and what are the ideal AP mobile platform configurations?* and 2) *Given the ideal configurations of the AP mobile platform, how much performance gain can be achieved by AP mobility in various scenarios (e.g., compared with static APs)?* The major contributions of this work are to investigate and answer these two fundamental questions using both simulation-based and theoretical analyses. While related works have explored a floor-based mobile AP that navigates its way around obstacles for conventional WiFi [2], [3], [5], we identify and propose a simpler but more effective model in this work - *a ceiling-mounted mobile (CMM) AP that moves on a linear actuator*. We first show through a simulation-based evaluation that the different configurations of the AP mobile platform do have a significant impact on the network performance. After identifying the ideal CMM AP platform configurations, we then use simulations to identify that a CMM AP performs better than as many as 5 ceiling-mounted static APs from the perspective of throughput and fairness. Finally, we use theoretical analysis to further confirm the potential gains of a CMM AP. In this work, as we identify there is a promising potential gain of the CMM AP, a systematic algorithm can then be correspondingly designed to leverage the benefits of AP mobility to optimize the overall performance for mmWave WiFi networks.

## II. NLOS ISSUE AND PROBLEM FORMULATION

### A. NLOS Issue In mmWave WiFi

The key advantage of mmWave WiFi compared to conventional WiFi is the availability of a massive amount of spectrum. However, achieving the multi-gigabit performance in mmWave WiFi is not a trivial problem, since the mmWave signal propagation characteristics significantly differ from that of the conventional frequency. The major difference is that mmWave communication suffers from *extremely high signal attenuation* [6] generally caused by: 1) high propagation loss: there is an additional signal attenuation of 22dB at 60GHz compared to that of 5GHz based on the free space path loss model and the properties of the propagation media can also significantly amplify the signal attenuation (e.g., oxygen absorption at 60GHz); 2) high penetration loss: the attenuation impact is significantly amplified when there is shadow fading or NLOS between the transmitter and receiver pair; and 3) sparse multipath diversity: multipath components propagating through objects tend to have low signal power due to longer propagation paths and additional reflection loss. Note that a consequent advantage of mmWave WiFi compared with conventional WiFi is that the high signal attenuation naturally lowers the probability of interference.

Given the harsh mmWave signal propagation characteristics, it is likely that robust wireless communication is hard to achieve. While beamforming can be utilized to combat the severe propagation loss in mmWave communication, the additional loss caused by NLOS can lead to severe performance degradation (e.g., a human blockage can lead to an additional  $\sim 30$ dB loss [7]). Note that for 802.11ad, a 2dB additional loss could lead up to 1Gbps performance drop when the modulation and coding scheme drops from 23 to 22 [8]. As LOS connectivity can provide an ideal channel condition, it becomes highly critical in mmWave WiFi. In a simple experiment to observe the impact of NLOS on mmWave WiFi network performance, we build a mmWave link using a TP-Link Talon AD7200 AP and an Acer Travelmate P648 laptop. We observe that obstacles such as a wall, a metal cabinet, and a cardboard box can degrade the link performance from 1Gbps to 0Gbps, 0Gbps, and 0.52Gbps, respectively. Even though LOS connectivity provides promising benefits for mmWave WiFi, achieving LOS connectivity is not a trivial problem. Typical indoor scenarios consist of randomly located obstacles with various dimensions that could potentially block the mmWave LOS communications. Besides, both the mmWave devices and the obstacles can be dynamic, which would prevent the possibility of predetermining the ideal AP location with LOS connectivity to STAs. Infrastructure mobility is a strategy which allows for changing the AP location adaptively to optimize LOS connectivity between AP and STAs. Thus, we consider infrastructure mobility as a promising candidate solution to improve the mmWave WiFi network performance.

### B. Problem Formulation and Scope

The network scenario considered in this work is a single room with a single CMM AP serving STAs. For both the AP

and STAs, we assume both 5GHz and 60GHz are available. A robotic actuator is available and can be mounted at any arbitrary location in the room. An AP is attached to the robotic platform and able to move to  $P$  discrete available positions on the platform. The power and the Ethernet cords are delivered to the AP through the robotic actuator. There are  $m$  static STAs that intend to connect with the AP using 60GHz. The information on STAs' intention to connect to the AP is communicated through 5GHz. The main metrics we focus on are **LOS** and **Throughput**. LOS connectivity between the AP and an STA is defined as a binary with 1 representing LOS and 0 representing NLOS. Throughput between the AP and an STA is measured as the goodput. For AP at location  $p$  (with  $p \in [0, P]$ ) on the platform,  $LOS_{i,p}$  and  $Thpt_{i,p}$  representing LOS and throughput between AP at location  $p$  and STA  $i$ , respectively. Within this scope, the objective of this work is to identify the ideal AP mobile platform configuration to enable infrastructure mobility and the corresponding potential performance gain compared with static APs.

## III. SIMULATION METHODOLOGY

To evaluate the performance of AP mobility quantitatively, we use the ns-3 simulator [9]. To incorporate the features of indoor configurations and 802.11ad, we make the following modifications to the default ns-3 simulator.

### A. Simulation of Indoor Scenarios

Due to the lack of an indoor scenario model (especially an obstacle model) in ns-3, we implemented the following indoor scenario features. A room is simulated as a specific three-dimensional space with a given obstacle distribution model. To simplify the simulations, we assume that the obstacles are modeled as cuboids, and they are placed on the floor, where the overlapping of obstacles is allowed to mimic complex cuboids-based obstacles. Typically, when an STA is communicating with an AP, it is located on the top of an obstacle (e.g., laptop on the desk) or attached to the side of an obstacle (e.g., TV on the wall). To simulate such practical scenarios, we consider that the placement of the STA follows an obstacle dependent distribution, where an obstacle is uniformly selected as the base location for the STA, and the STA is uniformly distributed on top or sides of the selected obstacles.

To accurately simulate the indoor obstacles, the implemented obstacle model has the following features:

- The center of the obstacles follows a Poisson point process (PPP) as shown in Eq. 1. The probability distribution for the number of obstacles to be uniformly placed in an indoor scenario is given as:

$$P\{N = n\} = \frac{\lambda^n * e^{-\lambda}}{n!} \quad (1)$$

where, the expected number of obstacles per unit area is defined as  $\lambda$  and  $n$  is the number of obstacles to be distributed.

- The  $x$ ,  $y$ , and  $z$  dimension of obstacles follow a truncated normal distribution to constrain the maximum and minimum of obstacle dimension.

TABLE I: Default Parameters

Parameter	Setting
Size of room (m)	(9, 4, 3)
$\lambda$	4.7
$(\mu_x, \mu_y, \mu_z)$ (m)	(0.54, 0.28, 0.61)
$(\sigma_x, \sigma_y, \sigma_z)$ (m)	(0.18, 0.08, 0.21)
Platform location	Center of the ceiling
Platform orientation	Parallel to shorter edge
Platform shape	Straight line
Platform length (m)	3
P	30
STA number	1
$n_{pl}$	2
$\sigma_m$	2.24

- The material of the obstacle is uniformly chosen from [10] to represent materials with various penetration losses.

We show the default parameters used in the simulation in Table I. The parameters are derived by using a real-life physical space (a lab environment) as a guiding example. To build a cuboid-based obstacle model, the  $x$ ,  $y$ , and  $z$  dimensions are collected based on the largest dimensions of a measured obstacle. We then collect the number of obstacles in the lab space as  $n$ . To calculate the  $x$ ,  $y$ ,  $z$  dimension distribution parameters, we use the distribution fitter in MATLAB to calculate the best fit normal distribution with mean  $\mu_x, \mu_y, \mu_z$ , and standard deviation  $\sigma_x, \sigma_y, \sigma_z$ . The maximum and minimum of  $x$ ,  $y$ , and  $z$  dimensions of obstacles are utilized as the range limits in the truncated normal distribution.

### B. Simulation of 802.11ad

We use the 802.11ad model based on [11]. The simulator provides all techniques that are essential for 802.11ad, such as beamforming training and steering, hence providing an accurate simulation environment for 802.11ad. The mmWave channel is another essential component of simulating the performance of 802.11ad. To incorporate shadow fading based on information of mmWave WiFi devices and obstacles, we consider the impact of shadow fading and multipath separately. Specifically, we modified the widely accepted log-distance based path loss model as follows:

$$L(d) = L(d_0) + 10 * n_{pl} * \log_{10}\left(\frac{d}{d_0}\right) + X_s + X_{\sigma_m} \quad (2)$$

where,  $L(d_0)$  is the path loss at a reference distance  $d_0$ ,  $n_{pl}$  is the path loss exponent,  $d$  is the distance between two communication devices,  $X_s$  represents shadow fading where the penetration loss is calculated based on the obstacles' location, dimension and material between mmWave WiFi devices, and  $X_{\sigma_m}$  represents the normally distributed multipath fading with  $\sigma_m$  as the standard deviation. Particularly,  $X_s$  is 0 when the communication link is in LOS connectivity. We collected the average of 5 sets of experimental estimations of the log-distance based path loss model to collect  $n_{pl}$  and  $\sigma_m$  based on [12], which are presented in Table I.

## IV. A SIMULATION-BASED STUDY OF AP MOBILITY

In this section, we use simulation analysis to identify the potential impact and benefits of AP mobility using the

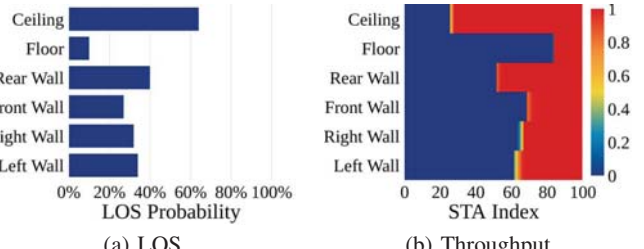


Fig. 1: AP Mobility: Floor vs. Walls vs. Ceiling

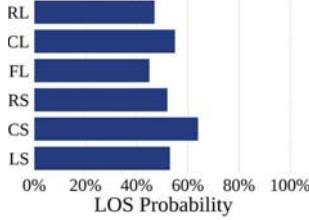
simulation platform described in the previous section. Specifically, considering the case of AP mobility, to evaluate the performance of a specific STA  $i$  with the mobile AP, we utilize the optimal LOS ( $\text{Max}_p(\text{LOS}_{i,p})$ ) and optimal throughput ( $\text{Max}_p(\text{Thpt}_{i,p})$ ), which represents the maximum LOS and throughput performance that can be achieved while AP is at location  $p$  on the mobility platform. In this context, we investigate 1) the impact of different AP mobile platform configurations on network performance, and 2) the performance of a CMM AP and multiple static APs.

### A. AP Mobility Platform Configurations

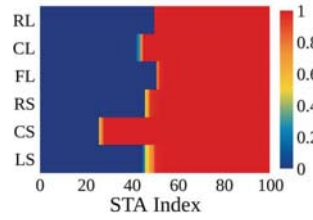
**AP Mobility - Floor vs. Walls vs. Ceiling:** Intuitively, as the platform is located on the ceiling, the expected LOS and throughput performance of the platform should be the best compared to the platform placed on the walls or the floor. We use quantitative simulation analysis to validate the above hypothesis and identify the corresponding performance gain of a CMM AP.

Fig. 1a illustrates the optimal LOS probability when the AP platform is located on the floor, the walls, and the ceiling. The expected optimal LOS probability of the CMM AP performs 88%, 100%, 137%, 60%, and 540% better compared with AP located on the left wall, the right wall, the front wall, the rear wall, and the floor, respectively. Clearly, the floor-based platform has the worst LOS performance due to the high probability of blockage. In this set of simulations, because of the specific randomly generated layout of obstacles, the AP mobile platform has relatively high performance when it is located on the rear wall compared with other walls. Similarly, Fig. 1b illustrates the throughput performance <sup>1</sup>. The expected optimal throughput of the CMM AP is 101%, 116%, 139%, 54%, and 460% better compared with AP located on the left wall, the right wall, the front wall, the rear wall, and the floor, respectively. The maximum achieved throughput performance is nearly 4Gbps. We observe that LOS performance is proportional to throughput performance. It is interesting to observe that the throughput performance is mostly either maximum or minimum. The reasons are that NLOS connectivity is likely to result in minimum performance due to high penetration loss, and LOS connectivity is likely to result in maximum performance due to the limited room size. In Section V, we use theoretical analysis to validate the relationship between LOS probability and the AP's height.

<sup>1</sup>The STA index in all figures is sorted in ascending fashion with respect to the metric being plotted for easier interpretation.



(a) LOS



(b) Throughput

Fig. 2: Comparison of Locations on Ceiling

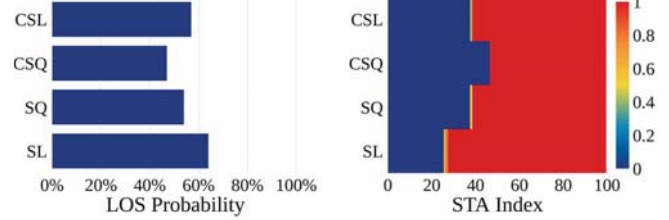
The performance of a CMM AP is significantly better than that of floor-based or wall-based AP mobility.

**Ceiling Location:** Based on the above simulation analysis, it is clear that a CMM AP achieves the best performance compared with other types of AP mobility. However, considering the default linear robotic platform, the orientation and location to place the platform is still an interesting problem to investigate. We use simulations to validate the expected optimal LOS and throughput performance when the platform is located on the edges and the center of the ceiling with the direction of the platform either parallel to the shorter edge or the longer edge. The specific instances of ceiling locations considered are: on the left shorter edge (LS), right shorter edge (RS), center parallel to the shorter edge (CS), front longer edge (FL), rear longer edge (RL), and center parallel to the longer edge (CL).

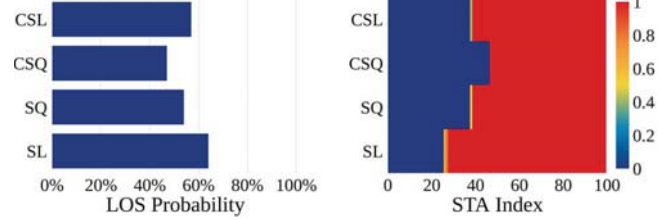
Fig. 2a and 2b show the optimal LOS probability and optimal throughput performance as the AP platform is located at the edges or the center of the ceiling with orientation parallel to the shorter edge or longer edge. Clearly, the CS based AP platform has optimal performance. There are 21%, 23%, 42%, and 36% LOS probability improvement of the CS based platform compared with LS, RS, FL, CL, and RL based platform, respectively. The throughput performance gain is observed to be proportional to LOS performance and follows a similar trend. Since the obstacles follow a PPP and the STAs follow an obstacle dependent distribution, the center-based CMM AP is more likely to have the largest LOS coverage area. Even considering the case with NLOS connectivity between the AP and STAs, the AP platform located at center benefits from shorter expected distance w.r.t. STAs. Thus, it leads to less expected propagation loss providing a higher margin at the receiver to compensate for the additional penetration loss. It is also interesting to observe that when the platform is parallel to the shorter edge, the performance is better than when the platform is parallel to the longer edge. We will validate that higher LOS probability can be achieved while the platform is parallel to the shorter edge of the room using theoretical analysis in Section V.

The performance of CS based CMM AP is better than that of other locations based CMM APs.

**Platform Shape:** The major advantage of AP mobility is the diversity in AP locations provided by the AP mobile platform. As the shape of the AP mobility platform can dramatically change the AP diversity locations, it can have significant impact on network performance. We herein investigate the



(a) LOS



(b) Throughput

Fig. 3: Comparison of Platform Shape

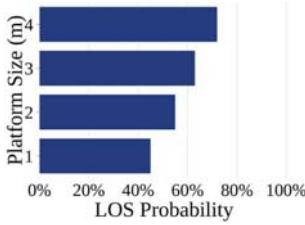
impact of different AP mobility platform shapes on the network performance. We consider 4 different platform shapes: 1) straight line (SL), where AP location diversity is along a single dimension, 2) cross straight line (CSL), with two perpendicular lines with the same length, 3) compressed square (CSQ), where the AP mobile platform has continuous movement range in a given square area, 4) Square (SQ), where the AP mobile platform can only move on the boundary of a given square area. Specifically, the total length for the AP mobile platform is fixed as 3m for all the platform shapes, and the width of the platform segment is 0.65m.

Fig. 3a and 3b present the optimal LOS and throughput performance of different platform shapes. The expected optimal LOS probability of the SL based CMM AP performs 19%, 36%, 12% better than SQ, CSQ, and CSL based CMM AP, respectively. Similarly, the throughput performance gain is proportional to LOS performance. Clearly, SL based CMM AP performs the best and CSQ based CMM AP performs the worst. If the diversity of AP locations is maximized, the overlapping coverage area of all the AP locations is minimized. For the CSQ based CMM AP, the AP mobile platform provides continuous movement range in a given square area, where the AP location diversity is minimized, which leads to a limited performance gain. On the other hand, the SL based CMM AP maximizes the AP location diversity in a linear fashion, which leads to significantly better performance gain compared with other platform shapes.

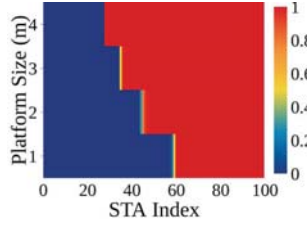
The performance of a SL based CMM AP is better than that of the other shapes based CMM AP.

**Platform Length:** Clearly, the larger the CMM AP platform is, the higher the potential AP location diversity can be provided, which can lead to a higher performance gain. The question we would like to investigate here is the performance gain when the platform length varies. Specifically, we change the platform length from 1m to 4m with steps of 1m.

Fig. 4a and 4b show the optimal LOS probability and throughput performance of different platform lengths. The performance of the CMM AP increases as the platform length increases. It is interesting to observe that the performance gain is not linearly proportional to the platform length. Specifically, the performance gain varies from 35%, 17%, and 12% when the platform length increases from 1m/2m/3m to 2m/3m/4m, respectively. As we identified within the ceiling location-based simulations, the AP mobile platform located at the edge of the ceiling leads to lower performance compared with the mobile



(a) LOS



(b) Throughput

Fig. 4: Comparison of Platform Length

AP located at the center of the ceiling. As the platform length increases towards the edge of the room, the performance gain per additional unit additional length decreases.

As the CMM AP platform length increases, the performance gain per additional unit length decreases.

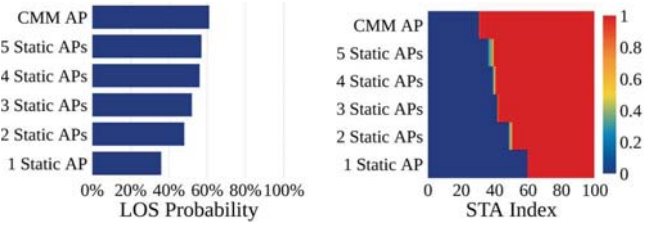
### B. A CMM AP vs. Static APs

**Single STA scenario:** After identifying that the platform configurations of a CMM AP can have a significant impact on network performance, we compare the performance of a CMM AP with ideal configurations with multiple static APs. The ideal CMM AP configurations follow the definition in Table I. A linear placement methodology is applied to place static APs on the ceiling. For a specific STA, we consider the maximum LOS and throughput performance achieved by one of the multi-AP as the performance of the multi-AP case. The number of static AP is set to be 1 to 5.

Fig. 5a and 5b show the expected optimal LOS and throughput performance of the CMM AP and static APs. We can observe that on an average the expected optimal LOS performance of CMM AP performs 92%, 44%, 33%, 23%, and 21% better than 1~5 static APs, respectively. Similarly, we can observe that on average expected optimal throughput performance of CMM AP performs 72%, 38%, 19%, 15%, and 12% better than 1~5 static APs, respectively. Clearly, both LOS and throughput performance of the CMM AP are better than 1~5 static APs. Specifically, the LOS and throughput performance of static APs increase as the number of static AP increases due to the improved AP location diversity. It is interesting to observe that the throughput performance of static APs increases by 25%, 16%, 3%, and 3% when the number of static APs increases from 1/2/3/4 to 2/3/4/5. We can observe that after the number of static AP reaches 3, the performance of static AP saturates due to the limited improvement of AP location diversity. Thus, the performance of the CMM AP with higher AP location diversity is better than as many as 5 static APs.

The performance of a CMM AP is better than that of 1~5 ceiling mounted static APs.

**Multi-STA scenario:** Other than throughput performance, network fairness is another essential metric for WiFi networks considering a multi-STA scenario. Fairness becomes even more critical in mmWave WiFi networks. Considering a 2-STA scenario, if the first STA is in NLOS with the AP



(a) LOS

(b) Throughput

Fig. 5: CMM AP vs. Multiple Static APs

and the second STA is in LOS with the AP, the aggregate network throughput performance will still be high. However, the STA in NLOS is likely to experience severely bad service quality. Thus, network fairness becomes a challenging issue to solve in mmWave WiFi as it is hard to guarantee the LOS connectivity between AP and all STAs. We will analyze both the throughput and fairness performance of the CMM AP and static APs in a multi-STA scenario. For simplicity, we assume only single AP is actively serving Multi-STA at a time without considering the problem of MAC sharing and optimum pairing between multi-AP and multi-STA. Specifically, we consider both optimal throughput and optimal Jain's fairness index ( $(Max_p(fairness_{i,p}))$ ) [13] for evaluations. For Jain's fairness index, it ranges from  $1/n_s$  (single STA has aggregate network throughput) to 1 (each STA has equal throughput), where  $n_s$  is the number of STA.  $n_s$  is set as 5.

Fig. 6a shows the aggregate optimal throughput performance of the CMM AP and static APs. The throughput performance of CMM AP outperforms 1~5 static APs are 76%, 35%, 7%, 4%, and 5%, respectively. The throughput performance of CMM AP is significantly better than static APs when the number of static AP is smaller than 3. As the number of static AP becomes larger than 3, the CMM AP performance gain is not significant. The reason is that as long as one STA among all STAs is in LOS with the AP, the throughput performance will be high. Thus, as the number of AP increases, it is likely that at least one STA is in LOS connectivity with one of the AP. To further analyze the network fairness, Fig. 6b presents the Jain's fairness index for CMM AP and static APs. The fairness performance of the CMM AP is 91%, 69%, 35%, 26%, and 28% better than 1~5 static APs, respectively. Although the throughput performance of the CMM AP is comparable to 4~5 static APs, the CMM AP can achieve better network fairness compared with static APs for the multi-STA scenario. The reason is that the CMM AP can provide the highest number of LOS connectivity with STAs due to the higher AP location diversity provided by the AP mobile platform.

A CMM AP can perform better than 1~5 static APs in the perspective of throughput and fairness.

### V. A THEORETICAL STUDY OF AP MOBILITY

In this section, we use stochastic geometric methods to evaluate the performance of the CMM AP theoretically. First, we analyze the LOS probability in terms of the heights of the AP and STAs and any obstacle between them as shown in Fig.

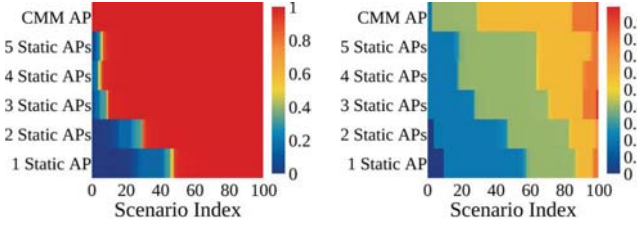


Fig. 6: Comparison of Multiple STAs

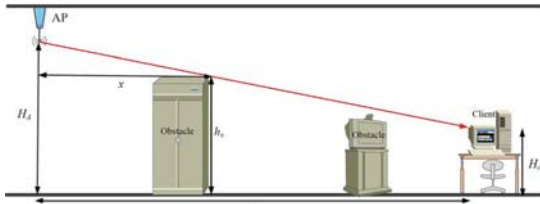


Fig. 7: Side view of a room

7. We know that an obstacle intersecting the link between AP and STA with a horizontal length of  $d$  blocks the LOS path if and only if its height  $h_o > h_x$ , where  $h_x = \frac{x}{d} \cdot (H_A - h_c) + h_c$ , and  $H_A$  and  $h_c$  are the heights of AP and STA, respectively.

We use  $B$  to denote the event that the LOS path between AP and STA is blocked. Assuming the heights of the obstacle  $h_o$  and STA  $h_c$  follow the uniform distributions  $U(a_o, b_o)$  and  $U(a_c, b_c)$ , respectively, the conditional probability that an obstacle blocks the LOS path is:

$$\varepsilon = \int_{-\infty}^{+\infty} P(B|h_c) \cdot f_H(h_c) dh_c = 1 - \frac{1}{4} \cdot \frac{2H_A - (b_c - a_c)}{b_o - a_o} \quad (3)$$

Note that  $\varepsilon$  is independent of the number of obstacles only when the intersections with obstacles form a PPP on the LOS path between the AP and the STA. Therefore, incorporating the height of obstacles only introduces a constant scaling factor  $\varepsilon$  to the results that without considering the height.

Based on the Boolean scheme [14] of rectangles for obstacles in 2D blockage model without height effects, we know that the blockage area between AP and the STA is:

$$S_b(w, l, \theta, r) = r \cdot (|\cos \theta| \cdot w + |\sin \theta| \cdot l) + w \cdot l \quad (4)$$

where  $w, l, \theta$  are the obstacle's width, length and orientation, respectively. In addition to the obstacle's basic parameters, we can see that the blockage area  $S_b$  is related to the distance  $r$  between AP and STA. With a randomly located STA, this distance can be varied from 0 to  $R$  in a specific room, where  $R$  is the achievable distance between the AP and that random STA, which can be computed as:

$$R = \max\{\sqrt{x_a^2 + y_a^2}, \sqrt{(x_a - r_l)^2 + y_a^2}, \sqrt{x_a^2 + (y_a - r_w)^2}, \sqrt{(x_a - r_l)^2 + (y_a - r_w)^2}\} \quad (5)$$

where  $x_a, y_a$  are AP's horizontal and vertical coordinates, and  $r_l, r_w$  are the length and width of the room ( $r_l \geq r_w$ ).

Here we assume obstacles form a Boolean scheme of rectangles, and their centers  $C_o$  of these rectangles form a

homogeneous PPP of density  $\lambda$ . The widths  $W_o$  and lengths  $L_o$  are assumed to be i.i.d. distributed and follow the normal distribution as  $\mathcal{N}(\mu_w, \sigma_w^2)$  and  $\mathcal{N}(\mu_l, \sigma_l^2)$ . The orientation  $\theta_o$  of every obstacle is assumed to be uniformly distributed in  $(0, 2\pi]$ . Let  $K$  be the total number of obstacles with random sizes that fall in their respective blockage areas  $S_b$ , and  $K(S_b) = \sum_{w, l, \theta} N(w, l, \theta)$ . According to the superposition theorem of the PPP,  $K$  is also Poisson distributed, and its expectation can be calculated as:

$$\begin{aligned} E[K] &= \sum_{w, l, \theta} K(w, l, \theta) \\ &= \int_0^R \left[ \frac{2}{\pi} \cdot \lambda \cdot (\mu_w + \mu_l) \cdot r + \lambda \cdot \mu_w \cdot \mu_l \right] \cdot f_D(r) dr \end{aligned} \quad (6)$$

where  $f_D(r)$  is the probability density function of the distance between AP and STA in a specific room. Since the AP's position  $(x_a, y_a)$  and the STA's position  $(x_c, y_c)$  are independent and assumed to follow the uniform distribution, i.e.,  $X \sim U(0, r_l)$ ,  $Y \sim U(0, r_w)$ , we calculate the convolution of event  $(X_a - X_c)^2$  and event  $(Y_a - Y_c)^2$  so that  $f_D(r)$  is:

$$f_D(r) = \begin{cases} \frac{2r^3}{r_w^2 r_l^2} - \left( \frac{4r^2}{r_w^2 r_l} + \frac{4r^2}{r_w r_l^2} \right) + \frac{2\pi r}{r_w r_l}, & 0 < r \leq r_w \\ -\frac{4}{r_w^2 r_l} \cdot r^2 - \frac{2}{r_l^2} \cdot r + \frac{4}{r_w r_l} \cdot r \cdot \arcsin\left(\frac{r_l}{r}\right) \\ + \frac{r_w^2 r_l}{r_w^2 r_l} \cdot r \cdot \sqrt{r^2 - r_w^2}, & r_w < r \leq r_l \\ -\left(\frac{2r}{r_w^2} + \frac{2r}{r_l^2}\right) + \frac{4r}{r_w r_l} \cdot [\arcsin\left(\frac{r_w}{r}\right) + \arcsin\left(\frac{r_l}{r}\right)] \\ + \frac{4}{r_w^2 r_l} \cdot r \cdot \sqrt{r^2 - r_w^2} + \frac{4}{r_w r_l^2} \cdot r \cdot \sqrt{r^2 - r_l^2} \\ - \frac{2\pi}{r_w r_l} \cdot r - \frac{2}{r_w^2 r_l^2} \cdot r^3, & r_l < r \leq \sqrt{r_w^2 + r_l^2} \end{cases} \quad (7)$$

Then, we incorporate the height effect of obstacles, and the LOS probability in terms of AP's location is obtained by substituting Eq. (3)-(7) into the following equation:

$$P_{LOS}(x_a, y_a) = \frac{[\lambda(x_a, y_a)]^n}{n!} e^{-\lambda(x_a, y_a)}|_{n=0} = e^{-\min\{\varepsilon, 1\} \cdot E[K]} \quad (8)$$

Note that the closed-form equation of  $E[K]$  is not listed here due to the space limitation, and it can be derived by calculating the integral of Eq. (6).

With this analytical result, we first investigate how the AP's height affects the LOS probability. According to Eq. (3) and (8), we observe that  $H_A$  is inversely proportional to  $\varepsilon$ , so  $P_{LOS}$  increases monotonically with increasing  $H_A$ . *It proves that the largest AP height provides the maximum LOS probability.*

Now, we consider how the LOS probability varies with different AP locations on the ceiling of a room. Fig. 8 shows LOS probability vs. AP's locations. *We identify that a linear CS based CMM AP can achieve the highest LOS probability.* Due to space limitations, we consider the theoretical analyses of the platform shape and length as further work.

## VI. RELATED WORK

As LOS connectivity becomes a critical bottleneck for mmWave communications, there are numerous research works that address this by proposing compensation methods. We categorize related works that have addressed the challenges

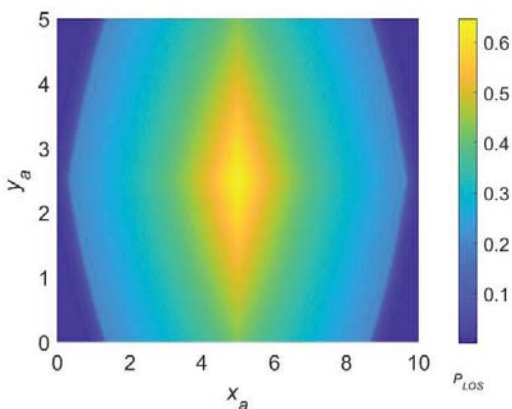


Fig. 8: LOS probability vs. AP's location

related to LOS connectivity into three types: 1) multi-band approach, 2) improving channel quality, and 3) establishing indirect LOS connectivity. In multi-band approaches, mmWave is only utilized for good (e.g, LOS) connections, and conventional band is utilized when the mmWave connections experience poor propagation (e.g., NLOS) conditions. [15] utilizes localization by tracking angle change to steer the beam to a new location for mobile STAs, and re-directing user traffic to a more robust wireless interface in the absence of LOS (e.g., from 60GHz to 5GHz). To provide good signal reception between AP and STAs, some possible approaches are: 1) infrastructure mobility: related works include [16] where robotic APs make adjustments to their positions to converge to an optimum position; 2) multiple APs: [17], [18] considers to deploy more than one AP in a single scenario to increase the probability of LOS between AP and STAs; and 3) relays: [19], [20] utilizes relays to improve signal quality at the receiver end. Of these, only infrastructure mobility can improve physical channel conditions dynamically.

The approach to establish indirect LOS connectivity between AP and STA typically requires modifications to the propagation environment, which can be infeasible [21].

## VII. CONCLUSIONS

In this work, we explore the use case of infrastructure mobility to provide the LOS connectivity to STAs within indoor mmWave WiFi networks. We make a detailed case for a CMM AP by comparing its performance with other types of AP mobility and multiple static APs. Through both simulation and theoretical analyses, we identified that the CMM AP is a promising strategy to improve the performance of mmWave WiFi. Given the benefits of infrastructure mobility, the following are the essential future work to be considered: 1) analyzing benefits of AP mobility in case of dynamic environment (e.g., moving STAs), 2) designing a systematic algorithm to leverage the benefits of AP mobility, and 3) AP mobility cost analysis.

## ACKNOWLEDGEMENT

This work was supported in part by the National Science Foundation under grants CNS-1513884, IIP-1701115, CNS-1813242, and CNS-1837369, and the Wayne J. Holman Chair.

## REFERENCES

- [1] Cisco visual networking index: Forecast and methodology 2017-2022, 2017. URL: <https://www.cisco.com/c/en/us/solutions/collateral/service-provider/visual-networking-index-vni/white-paper-c11-741490.html>.
- [2] Mahanth Gowda, Ashutosh Dhekne, and Romit Roy Choudhury. The case for robotic wireless networks. In *Proc. of 25th International Conference on World Wide Web*, pages 1317–1327, 2016.
- [3] Yubing Jian, Shruti Lall, and Raghupathy Sivakumar. Toward a self-positioning access point for wifi networks. In *Proceedings of the 16th ACM International Symposium on Mobility Management and Wireless Access*, pages 19–28, 2018.
- [4] Yubing Jian, Mohit Agarwal, Yuchen Liu, Douglas M Blough, and Raghupathy Sivakumar. Poster: Hawkeye-predictive positioning of a ceiling-mounted mobile ap in mmwave wlans for maximizing line-of-sight. In *Proceedings of the 25th ACM International Conference on Mobile Computing and Networking*, pages 1–3, 2019.
- [5] Yubing Jian, Shruti Lall, and Raghupathy Sivakumar. Poster: Twirl: On the benefits of adapting orientation of a wifi access-point. In *Proceedings of the 15th ACM Annual International Conference on Mobile Systems, Applications, and Services*, pages 174–174, 2017.
- [6] Hao Xu, Vikas Kukshta, and Theodore S Rappaport. Spatial and temporal characteristics of 60-ghz indoor channels. *IEEE Journal on selected areas in communications*, 20(3):620–630, 2002.
- [7] Sanjib Sur, Vignesh Venkateswaran, Xinyu Zhang, and Parmesh Ramanathan. 60 ghz indoor networking through flexible beams: A link-level profiling. 43(1):71–84, 2015.
- [8] Ieee standard 802.11ad-2012, 2012. URL: <https://ieeexplore.ieee.org/stamp/stamp.jsp?arnumber=6392842>.
- [9] ns-3. URL: <https://www.nsnam.org/>.
- [10] Jonathan Lu, Daniel Steinbach, Patrick Cabrol, Phil Pietraski, and Ravikumar V Pragada. Propagation characterization of an office building in the 60 ghz band. In *Proc. of 8th European Conference on Antennas and Propagation*, pages 809–813, 2014.
- [11] Hany Assasa and Joerg Widmer. Implementation and evaluation of a wlan ieee 802.11 ad model in ns-3. In *Proceedings of the Workshop on ns-3*, pages 57–64, 2016.
- [12] Peter FM Smulders. Statistical characterization of 60-ghz indoor radio channels. *IEEE Transactions on Antennas and Propagation*, 57(10):2820–2829, 2009.
- [13] Rajendra K Jain, Dah-Ming W Chiu, and William R Hawe. A quantitative measure of fairness and discrimination. *ACM Transactions on Computer Systems*, pages 2–7, 1984.
- [14] Tianyang Bai, Rahul Vaze, and Robert W Heath. Analysis of blockage effects on urban cellular networks. *IEEE Transactions on Wireless Communications*, 13(9):5070–5083, 2014.
- [15] Sanjib Sur, Ioannis Pefkianakis, Xinyu Zhang, and Kyu-Han Kim. Wifi-assisted 60 ghz wireless networks. In *Proceedings of the 23rd Annual International Conference on Mobile Computing and Networking*, pages 28–41, 2017.
- [16] Stephanie Gil, Swaran Kumar, Dina Katabi, and Daniela Rus. Adaptive communication in multi-robot systems using directionality of signal strength. *The International Journal of Robotics Research*, 34(7):946–968, 2015.
- [17] Sanjib Sur, Ioannis Pefkianakis, Xinyu Zhang, and Kyu-Han Kim. Towards scalable and ubiquitous millimeter-wave wireless networks. In *Proceedings of the 24th Annual International Conference on Mobile Computing and Networking*, pages 257–271, 2018.
- [18] Yuchen Liu, Yubing Jian, Raghupathy Sivakumar, and Douglas M Blough. Optimal access point placement for multi-ap mmwave wlans. In *Proceedings of the 22nd ACM Conference on Modeling, Analysis and Simulation of Wireless and Mobile Systems*, pages 35–44, 2019.
- [19] Yan Yan, Qiang Hu, and Douglas M Blough. Path selection with amplify and forward relays in mmwave backhaul networks. In *IEEE 29th Annual International Symposium on Personal, Indoor and Mobile Radio Communications (PIMRC)*, pages 1–6, 2018.
- [20] Yan Yan, Qiang Hu, and Douglas M Blough. Optimal path construction with decode and forward relays in mmwave backhaul networks. In *Proceedings of the IEEE International Conference on Computing, Networking and Communications*, 2020.
- [21] Xia Zhou, Zengbin Zhang, Yibo Zhu, Yubo Li, Saipriya Kumar, Amin Vahdat, Ben Y Zhao, and Haitao Zheng. Mirror mirror on the ceiling: Flexible wireless links for data centers. *ACM SIGCOMM Computer Communication Review*, 42(4):443–454, 2012.